JOURNAL OF GUIDANCE, CONTROL, AND DYNAMICS
Vol. 22, No. 6, November–December 1999

Longitudinal Landing Control Law for an Autonomous Reentry Vehicle

Yoshikazu Miyazawa* and Toshikazu Motoda†
National Aerospace Laboratory, Chofu, Tokyo 182-8522, Japan
Tatsushi Izumi‡
National Space Development Agency of Japan, Chofu, Tokyo 182-8522, Japan
and
Takashi Hata§
Mitsubishi Heavy Industries Company, Ltd., Nagoya 455-8515, Japan

This paper discusses the longitudinal flight-path control law designed and flight tested for the Automatic Landing Flight Experiment (ALFLEX). ALFLEX, for which flight tests were conducted in 1996, demonstrated Japanese potential for developing automatic landing technology for a reentry space vehicle. One of the critical factors in satisfying the design requirements for landing on a limited length runway was longitudinal flight-path control following the preflare maneuver. Robustness against uncertainties and sensor errors is a key issue in longitudinal flight-path control. The longitudinal guidance and control laws were carefully designed and flight tested. Although the flight tests proved that the design satisfied all landing requirements, it identified critical parameters affecting landing performance such as vehicle longitudinal aerodynamics, navigation error, and air data sensor error. This paper describes data obtained during the development and flight tests, as well as further investigations conducted after the flight tests in order to improve landing performance for future space vehicle developments. In the subsequent design review a new approach called stochastic gain tuning was adopted, where the guidance feedback gain is tuned to maximize the probability of mission success. The results indicate some possibility of improvement of robustness.

Nomenclature

C_D	= drag coefficient
$C_{D_{\delta sb}}$, $C_{m_{\delta sb}}$	= drag and pitching moment coefficients per speedbrake angle
C_L	= lift coefficient
C_{L_α}, C_{m_α}	= lift and pitching moment coefficients per angle of attack
$C_{L_{\delta e}}$, $C_{m_{\delta e}}$	= lift and pitching moment coefficients per elevator angle
C_m	= pitching moment coefficient
C_{m_q}	= pitching moment coefficient caused by pitch rate
G	= 1 G constant, m/s^2
h, $\dot{h}$	= altitude, m, and rate, m/s
h_{gear}	= altitude of main landing gear, m
h_{ref}, $\dot{h}_{\text{ref}}$	= reference altitude, m, and rate, m/s
I_{yy}	= moment of inertia about body Y axis, kgm^2
Kp, Kd	= proportional and derivative feedback gains
n_c	= acceleration command normal to velocity vector, G
q_{cmd}	= pitch rate command, rad/s
q_v	= dynamic pressure, Pa
q_{50}	= dynamic pressure of $V_{\text{EAS}} = 50$ m/s, Pa
V_{EAS}	= equivalent air speed, m/s
V_G	= ground speed, m/s
V_{ref}	= reference equivalent air speed, m/s
V_{sink}	= sink rate, vertical velocity ($=\mathrm{d}Z/\mathrm{d}t$), m/s
X, Y, Z	= vehicle's position in runway coordinate frame, m
X_{stop}	= stop position's X coordinate, m
α	= angle of attack, rad
β_G	= inertial velocity vector's side-slip angle, deg
γ, γ_{ref}	= path angle and reference, rad
Δaz_{cmd}	= acceleration command, body axis, m/s^2
Δh, $\Delta \dot{h}$	= altitude error and rate, m, m/s
Δt_G	= time step for guidance calculation, s
δ_e, $\delta_{e_{\text{cmd}}}$	= elevator angle and command, rad
δ_{sb}, $\delta_{\text{sb}_{\text{cmd}}}$	= speedbrake angle and command, rad
σ	= standard deviation
Φ, Θ, Ψ	= attitude, Euler angles, rad

Subscripts

cmd	= command
f	= filter output
max	= maximum
ref	= reference

I. Introduction

THE U.S. space shuttle is a unique operational winged reentry space vehicle and is a proven technology for space vehicle atmospheric flight and horizontal landing.[1–9] In Japan the National Aerospace Laboratory (NAL) and the National Space Development Agency of Japan (NASDA) have been collaboratively conducting research to acquire key technologies necessary for future reentry space vehicle developments. The H-II Orbiting Plane Experiment (HOPE-X) program was started in 1996 to fully establish reentry space vehicle technology from launch to landing, in which the HOPE-X vehicle was intended to be the prototype of a follow-on H-II Orbiting Plane (HOPE). Although the HOPE program has recently been canceled in favor of research into future reusable launch vehicles, the HOPE-X program is continuing as an essential step in Japanese technological development.

Prior to the start of the HOPE-X program, scale-model flight experiment programs were conducted to acquire critical technologies. The Automatic Landing Flight Experiment (ALFLEX) is one of these.[10] Its purpose was to acquire reentry space vehicle subsonic flight control and automatic landing technology. Because the

Presented as Paper 98-4428 at the AIAA Guidance, Navigation, and Control Conference, Boston, MA, 10–12 August 1998; received 14 October 1998; revision received 30 March 1999; accepted for publication 14 April 1999.

*Head, Guidance and Control Laboratory, Flight Division. Member AIAA.
†Research Engineer, Flight Division. Member AIAA.
‡Associate Senior Engineer, Winged Space Vehicle Office; currently Deputy Director, Space Policy Division, Science and Technology Agency, Tokyo 100-8966, Japan.
§Manager, Space Electronics Designing Section. Member AIAA.

HOPE-X vehicle will be unmanned and autonomous, depending heavily on onboard computers, the guidance, navigation, and control (GNC) system is one of its most important components. To meet especially the demands of landing, the GNC system requires great accuracy and high tolerance against adverse conditions, such as wind and turbulence disturbance, sensor errors, uncertainties in flight characteristics and so on.[11]

The ALFLEX program started in 1992 and resulted in 13 landing flights being successfully conducted at Woomera, Australia, from 6 July to 15 August 1996 (Ref. 12). Figure 1 shows a photograph of the ALFLEX vehicle just after release from hanging equipment by which it is suspended from the helicopter mother ship. Many lessons were learned from the GNC system development and flight test, one of the most important of which was in longitudinal flight-path control. Although the longitudinal flight control design was carefully conducted to obtain the accurate-path following required for successful mission achievement, the obtained margin was critical. This paper focuses on the longitudinal flight guidance and control problem. It describes the process of the design, the development proceeding to the first landing trial, the lessons learned from the flight tests, and the results of further investigations carried out after the flight tests.

Regarding longitudinal flight characteristics, ALFLEX and HOPE-X differ from the U.S. space shuttle orbiter in the following respects:

1) The vehicle's maximum lift-to-drag ratio is 4.2, which is about 10% lower than that of the shuttle. Furthermore, because the planned HOPE-X's wing loading is about 60% of that of the shuttle, HOPE-X is more susceptible to wind. These factors result in a deeper glide slope angle and shorter length of shallow glide phase; consequently, HOPE-X's path following error in the preflare phase would be greater than the shuttle's, and it cannot be reduced in the shallow glide slope phase.

2) From the first flight the runway length is limited; in other words, the vehicle must be able to demonstrate required landing performance from the first flight.

This paper is organized as follows. The ALFLEX program is briefly reviewed in Sec. II. Section III describes details of the ALFLEX longitudinal guidance and control law examined by the flight tests. Section IV discusses the longitudinal path-following performance estimated in the preflight simulation analyses and the flight test results and summarizes key points of the longitudinal flight guidance and control problem, that is, that path-following performance is sensitive to errors in the vehicle's dynamics and sensors. Section V discusses results obtained from further investigations after the flight tests, that is, possible modifications to improve performance and their effects. These might not be evaluated by further flight tests, but can be evaluated by a simulation model validated by the ALFLEX flight tests.

Fig. 1 ALFLEX vehicle at release for landing flight.

II. ALFLEX Overview

ALFLEX is an experimental scale model of a future possible 15-ton-class space vehicle called HOPE.[10] Figure 2 shows three views of the ALFLEX vehicle. The vehicle airframe is designed to be dynamically similar to the HOPE candidate studied in 1992, with a scale of length of 37%. For HOPE to land on a standard size 3000-m-class runway, the runway length for ALFLEX was specified as 1000 m. The vehicle's mass is 796 kg, against a design target mass of 760 kg. To simulate HOPE's approach and landing phase, the vehicle is lifted to an appropriate position and an altitude of 1500 m by helicopter, from which it is dropped and then proceeds in automatic free flight toward the runway, controlled by an onboard flight control system.

A. GNC System

The GNC system for ALFLEX is also designed to be as similar as possible to that of the final HOPE vehicle. Table 1 shows the design requirements. Automatic landing performance is evaluated mainly from parameter values at touchdown. The GNC system was designed to satisfy the requirements under appropriately defined wind conditions, which were derived from HOPE's design wind conditions by the similarity rule. The ALFLEX vehicle has avionics similar to the future HOPE vehicle, i.e., commercially proven avionics and off-the-shelf components are installed. Because of the experiment characteristics, and for simplicity, all components are single channel, and there is no redundancy except for an emergency flight termination system.

Figure 3 shows a simple function block diagram of ALFLEX's GNC system. The Flight Control Program (FCP) was developed to provide the GNC function. For navigation the flight control

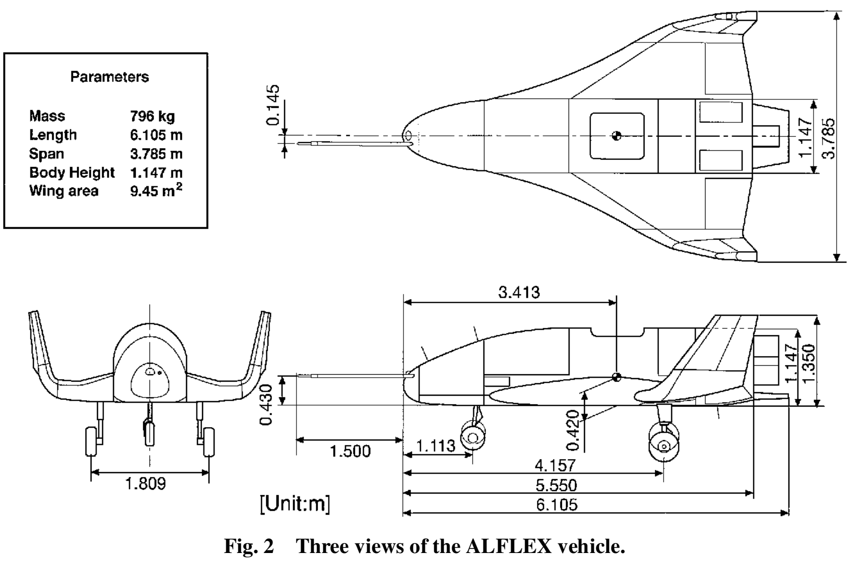

Fig. 2 Three views of the ALFLEX vehicle.

computer (FCC) derives position and velocity estimates by inertial navigation, updating these estimates by appropriately selecting landing navigation aids such as the differential global positioning system (DGPS), microwave landing system (MLS), and radar altimeter (RA). Two integrated inertial navigation algorithms were developed: DGPS/IMU (inertial measurement unit) navigation and MLS/RA/IMU navigation. Because the DGPS performance had not been proven when the ALFLEX program started, real-time navigation was used only in the nonflight critical phase, the navigation algorithm being switched from DGPS/IMU to MLS/RA/IMU 20 s prior to release of the ALFLEX vehicle. The 3σ accuracy goals for the position and velocity estimates of DGPS/IMU navigation are 25 m and 0.5 m/s, respectively, in each axis. MLS/RA/IMU navigation provides estimates of the vehicle's position and velocity during free flight, with 3σ accuracy goals of 60, 8, and 0.8 m at touchdown for down range, lateral deviation, and altitude, respectively. RA is used from the altitude of 200 m.

The ALFLEX bare airframe's flight dynamics are unstable in both longitudinal and lateral rotational motions. For example, during the glide-slope-phase longitudinal static stability is negative, the time to double amplitude of its unstable mode being 0.8 s, and the lateral-directional motion has an unstable oscillatory mode with a natural frequency of 0.1 Hz and a time to double amplitude of 3 s. ALFLEX's flight characteristics change with angle of attack and have a certain range of uncertainty. Under these adverse control properties the flight control system should give sufficiently quick response to guidance commands to attain the required landing accuracy. The higher the feedback gain, however, the more vulnerable the system is to coupling with structural flexibility. The tradeoff between control performance and robustness is another critical issue in the ALFLEX GNC design, especially in the lateral axis.

The multiple delay model and multiple design point (MDM/MDP) approach developed at NAL and the H-infinity exact model matching (H_∞EMM) design method developed by MHI (Mitsubishi Heavy Industries Co., Ltd.) were applied to this design challenge.[13,14] The former approach derives a practical fundamental control law by simply representing high-frequency uncertainties by delay models. The latter method is then applied to enhance the robustness of this fundamental control law by using a high-order filter, which shapes the frequency response of the closed-loop transfer function. The ALFLEX longitudinal and lateral-directional control laws were realized by fifth and tenth order filters, respectively. The longitudinal control law will be discussed in greater detail in Sec. III.

Table 1 Landing performance requirements

Evaluation point	GNC requirement
Touch down position[a]	$X > 0$ m, $\lvert Y \rvert < 18$ m
Velocity	43 m/s $< V_{\mathrm{EAS}} <$ 59 m/s
	$V_G < 62$ m/s, $V_{\mathrm{sink}} < 3$ m/s
Attitude	$\Theta < 23$ deg, $\lvert\Phi\rvert < 10$ deg, $\lvert\Psi\rvert < 8$ deg
Side-slip	$\lvert\beta_G\rvert < 8$ deg
Ground roll position	$X_{\mathrm{stop}} < 1000$ m, $\lvert Y_{\max}\rvert < 20$ m

[a](X, Y, Z) is a runway coordinate system. The origin is at the runway threshold. The X axis is on the runway centerline, and the Z axis is directed downward.

B. Experimental System

Ground facilities such as MLS and DGPS ground stations, a flight data monitoring system, and laser tracker and tracking radar systems supported the experiment. The flight data monitoring system on the ground monitored the vehicle's status. The laser tracker provides reference vehicle position data for evaluation of the navigation system. The tracking radar provides position data for the flight safety monitoring system. Figure 4 shows the vehicle reference trajectory.

The mother ship helicopter is an important component of the experiment system. It carries onboard control/monitor equipment that can change the flight control computer's experiment mode. Furthermore, it has a unique configuration for flight testing, the so-called five degrees of freedom (DOF) hanging flight configuration shown in Fig. 5. The ALFLEX vehicle is attached to its towing cable at a gimbal at its c.g., and the hanging equipment has a winch by which the towing cable can be extended to a length of 4 m. In five DOF hanging flight the vehicle is constrained only in the direction of the cable. Because the vehicle's dynamics are close to those of free flight in a certain range of frequencies, the same free flight control law for rotational motion can be used for this configuration. The onboard flight control program has a function for generating various patterns of commands to evaluate the flight control system's function, the closed-loop system's stability, and the vehicle's aerodynamic characteristics in this configuration.[15,16] One of the most important objectives is to confirm lateral-directional stability. A series of preliminary hanging flight tests were conducted to enhance the probability of success of the first landing trial.

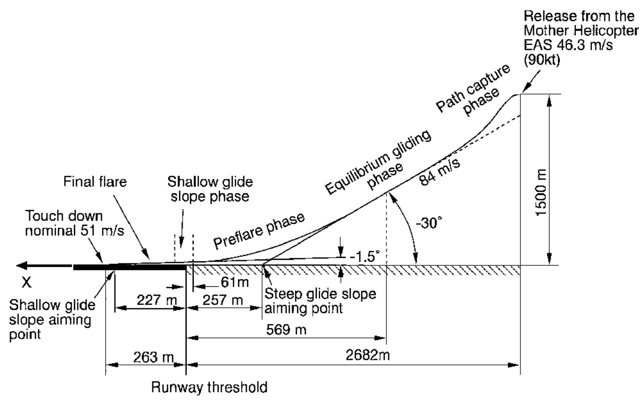

Fig. 4 Reference trajectory.

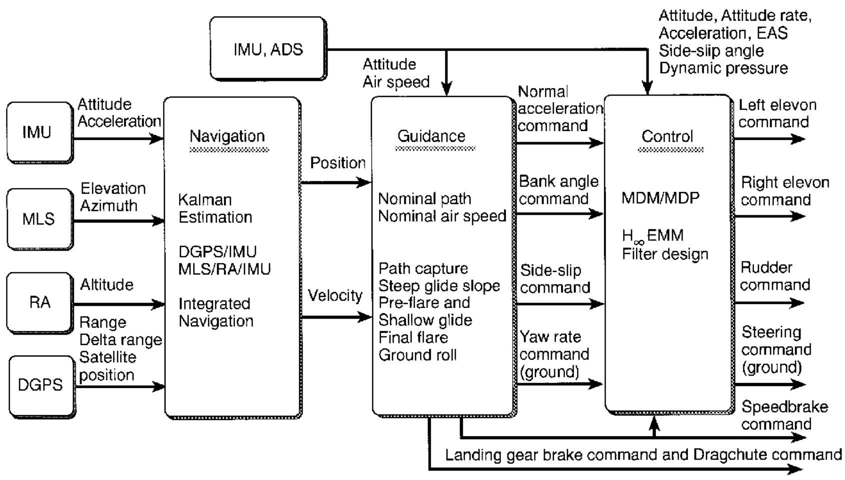

Fig. 3 GNC system function block diagram.

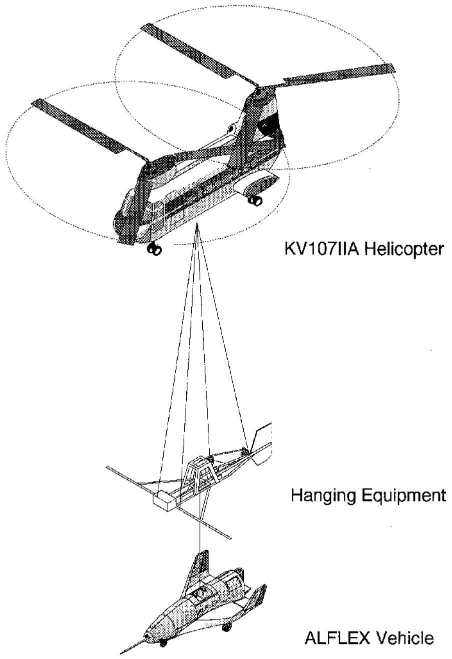

Fig. 5 Five DOF hanging flight configuration.

III. ALFLEX Longitudinal Guidance and Control

The objectives of longitudinal guidance are path following and equivalent air speed (EAS) keeping. Each objective is accomplished by generating corresponding longitudinal guidance commands; path following is achieved by a vertical acceleration guidance command, and velocity is controlled by a speedbrake command. The reference altitude and velocity are given as functions of range, or X position, with respect to runway axes.

Figure 6 shows the path-following and velocity guidance laws with reference altitudes. The path-following guidance laws differ between flight phases, such as equilibrium steep glide slope, preflare and shallow glide, and final flare. In the equilibrium steep glide slope flight phase, the guidance law is a simple proportional-integral-derivative (PID) control with constant gains. In the preflare and shallow glide slope phase, an open-loop command that corresponds to necessary vertical acceleration in the nominal condition is added to the feedback control. In the final flare phase the reference path is not used, but only sink rate is controlled as a function of altitude. The velocity guidance law is a simple proportional-integral (PI) feedback control with constant gains as shown in Fig. 6. The feedback gains were designed using linear models of point mass approximation. These were determined using the MDM/MDP approach by assuming appropriate design points and delay times for the vehicle's rotational response, e.g., three different velocity equilibrium points of 60, 80, and 100 m/s for the design points, and 1.5 s and none for the delay times,[13] and were then adjusted by trial and error with flight simulation analysis.

Longitudinal control (as opposed to guidance) stabilizes the vehicle's attitude and controls the vehicle's normal acceleration to follow the guidance command by deflecting the aerodynamic control surfaces (in fact, symmetrical actuation of elevons in place of true elevators). The longitudinal control law is common to all free flight phases. The total gain, however, is scheduled by an inverse of the measured dynamic pressure to compensate for changes in the effectiveness of the aerodynamic control surfaces. Because the elevon has a sufficiently large effect on pitching moment and the vehicle's pitch instability is mild (e.g. is 4% mean aerodynamic chord (MAC) aft of the aerodynamic neutral point in the most rearward case), pitch attitude control is not so difficult compared with lateral-directional control. The pitch rate controller is realized by a fifth-order feedback filter of a discrete state space form. The filter's constant gain was designed by the MDM/MDP and H_∞EMM methods.[14]

As it is shown in Fig. 7, the ALFLEX longitudinal control law has a unique structure in that the vertical acceleration command is transformed to a pitch rate command by an appropriate second-order

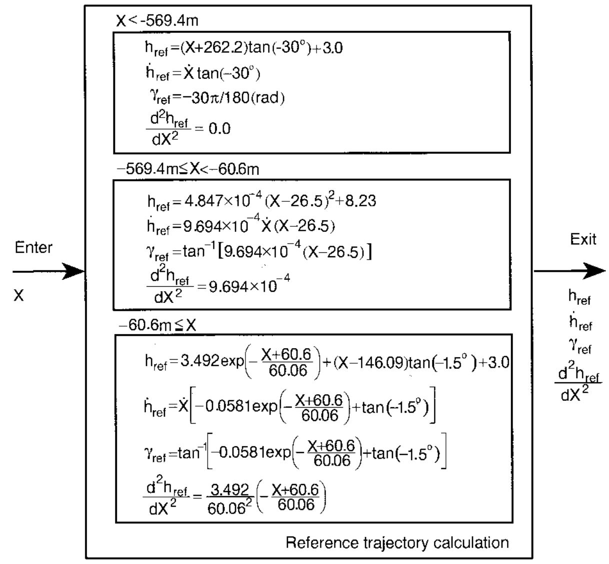

Fig. 6a Longitudinal guidance law (1).

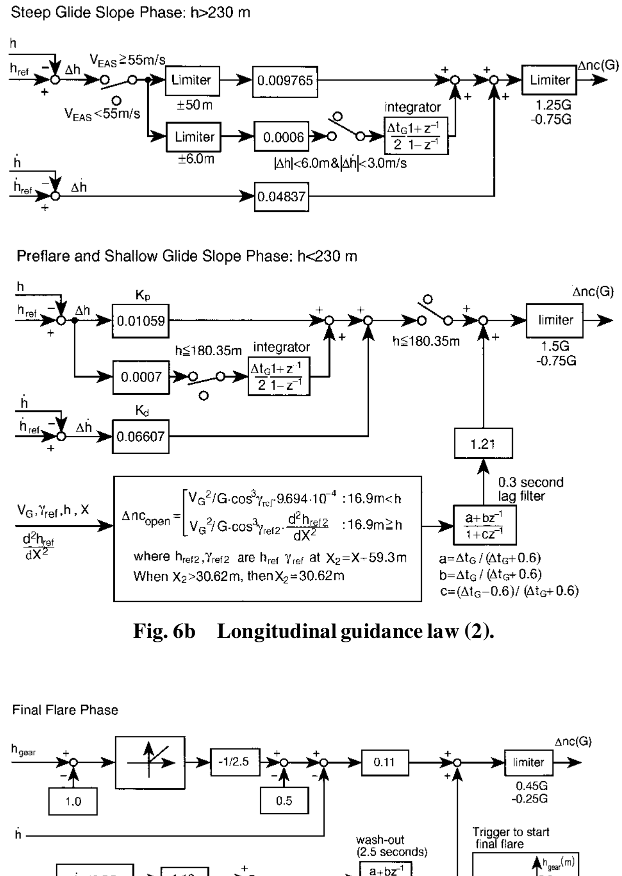

Fig. 6b Longitudinal guidance law (2).

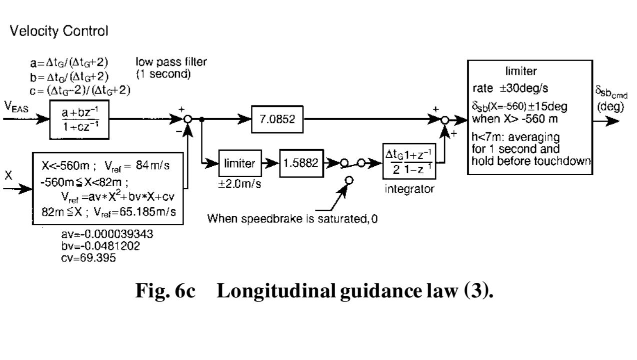

Fig. 6c Longitudinal guidance law (3).

precompensator. The precompensator does not use measured acceleration, but the filter dynamics are changed according to measured EAS. The precompensator's transfer function incorporates a lead function to achieve a quick acceleration response. This control structure can give rapid vehicle control response because standard acceleration feedback with relatively high gain often causes control/structure unstable oscillation, which limits the feedback gain even in the low-frequency range of rigid body motion. The precompensator's static gain is $(1/V_{EAS})$, but the V_{EAS} is estimated from an air data sensor and therefore inevitably contains some bias error. This point will be discussed later in Sec. V.

IV. ALFLEX Simulation and Flight-Test Results

A. Simulation Analysis Prior to the Flight Tests

Numerical flight simulation played a very important role in the ALFLEX program.[17,18] Because the vehicle is autonomous and fully automatic, controlled neither manually nor remotely, simulation is simpler than for a pilot-in-the-loop vehicle and can be carried out computationally off line. Uncertainties such as sensor error, aerodynamic characteristics, actuator dynamics, environmental conditions and so on, have been modeled by using approximately 100 variable parameters. In general, the probability distributions of each of these parameters are difficult to define, but in the ALFLEX simulations 3σ guidelines for each parameter were defined. For the aerodynamic characteristics, which are the most influential errors, the 3σ values are derived from shuttle design data.[19] The 3σ values of sensor and actuator errors are defined using specifications for each component, and those for wind, turbulence, and other environmental conditions are defined as design conditions. For other miscellaneous items the 3σ values are defined based on analysis and empirical data. Furthermore, for simplicity the assumption was made that in most cases each parameter's probability distribution is Gaussian and that parameters are independent of each other. Table 2 shows typical parameters affecting the longitudinal performance and their 3σ values. After defining the parameters' probability distributions, root-sum-square (RSS) and Monte Carlo simulation analyses were conducted.

RSS analysis estimates the approximate total error by summing the contributions of each parameter. Figure 8a is a typical example of an RSS analysis. Variations of touchdown position X and sink rate $\mathrm{d}Z/\mathrm{d}t$ are examined for each parameter's 3σ variation, and the largest 12 variations are plotted. The nominal touchdown position is $X = 292$ m, and the 3σ variation because of all of the uncertainties is 279 m. The requirement of $X > 0$ m (touchdown beyond the runway threshold) is barely satisfied. Here, the nominal condition refers to simulation using the most probable values of parameters.

Concerning the touchdown sink rate, the robustness is not sufficient, and the probability of exceeding the requirement, $\mathrm{d}Z/\mathrm{d}t < 3$ m/s, is not negligible. RSS analysis showed that the error in pitching moment vs angle of attack is the most influential factor affecting the performance. The charts in Fig. 8b shows the results of analyses by Monte Carlo simulation, where each dot corresponds to a result derived from one landing simulation. The right-hand chart shows values of $\mathrm{d}Z/\mathrm{d}t$, and in this example the landing simulation result exceeded the touchdown sink rate requirement in 39 out of 1000 cases. The left-hand chart shows the results for the touchdown position X and Y, with the origin at the runway threshold and the X axis pointing down the centerline. Although not as critical as the

Table 2 Typical uncertain parameters and their variations (most effective items for longitudinal landing performance)

Uncertain parameter	3σ value
C_{m_α}	0.00211, 1/deg
C_{L_α}	0.007, 1/deg
X_{nav}, Z_{nav} (initial)	25, m
θ bias	0.153, deg
$(\mathrm{d}X/\mathrm{d}t)_{nav}$, $(\mathrm{d}Z/\mathrm{d}t)_{nav}$ (initial)	0.5, m/s
Ground effect	100, %
MLS delay	46.5, ms
$C_{m_{\delta e}}$	0.001046, 1/deg
V_{EAS} bias	2, m/s
C_L	0.0216
Mass	24, kg
C_{m_q}	100, %
RA scale factor	3.1, %
RA bias	2, m
Temperature	10, deg
β bias	0.9, deg
I_{yy}	200, kgm^2

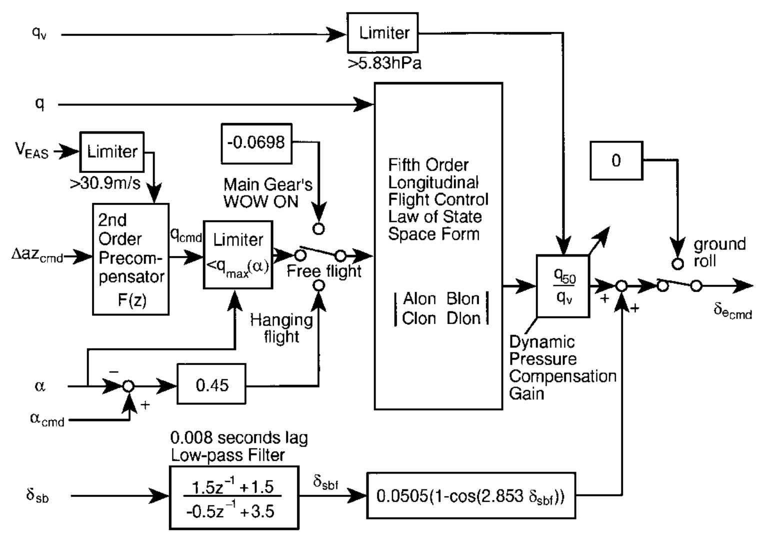

$$\begin{vmatrix} \mathrm{Alon} & \mathrm{Blon} \\ \mathrm{Clon} & \mathrm{Dlon} \end{vmatrix} =$$

1.0000E+00	0.0000E+00	0.0000E+00	0.0000E+00	0.0000E+00	4.0552E+01	-4.0552E+01
1.2499E-02	9.9968E-01	-7.1660E-02	-9.6801E+00	0.0000E+00	5.7148E+01	-4.8426E+01
7.6865E-05	1.2115E-02	9.1472E-01	-1.1547E+01	0.0000E+00	1.5855E+01	-2.9745E+00
2.5654E-07	5.6807E-05	7.6738E-03	3.1475E-01	0.0000E+00	3.1194E-01	-4.1821E-02
0.0000E+00	0.0000E+00	0.0000E+00	1.0000E+00	2.8000E-01	0.0000E+00	-6.6992E-02
0.0000E+00	0.0000E+00	0.0000E+00	3.6000E-01	4.6080E-01	0.0000E+00	-2.4117E-02

$$F(z) = \frac{(0.00177+0.2779\,\varepsilon)z^{-1} + (0.001704-0.2779\,\varepsilon)}{z^{-2} - 1.8817\,z^{-1} + 0.8852}\left(\frac{-1}{V_{EAS}}\right), \quad \varepsilon = 1/(0.03325V_{EAS} - 0.947)$$

Fig. 7 Longitudinal control law.

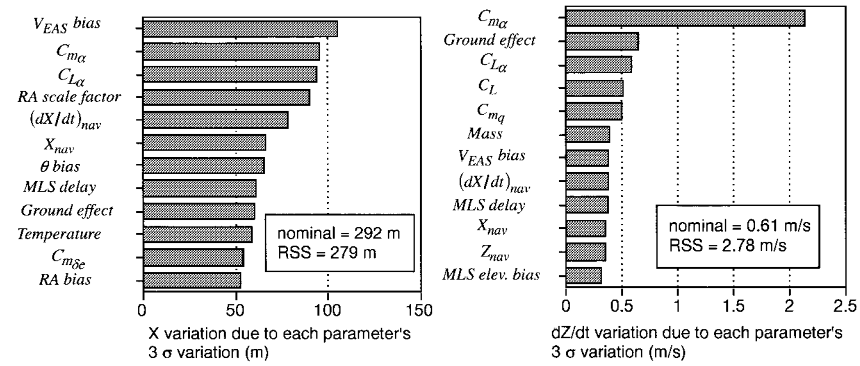

Fig. 8a RSS results (touch down position *X* and touch down sink rate d*Z*/d*t*).

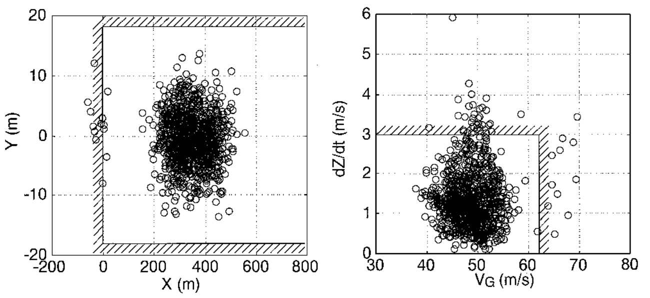

Fig. 8b Monte Carlo simulation results (prior to C_{m_α} and C_{L_α} variation reduction).

sink rate, the deviation of the touchdown position was larger than expected.

The RSS value for the touchdown sink rate and the probability of exceeding the requirement were difficult to accept because these results were obtained a few months before the scheduled first landing flight date following completion of the development phase of the program. One solution was to redesign the longitudinal guidance and control law, which would introduce some delay and change to the program schedule. Another solution was to reduce the variation of the longitudinal aerodynamic coefficients, for example, the 3σ values of the pitching moment and lift coefficient derivatives, by another validation method. As was mentioned in Sec. II.B, the preliminary hanging flight tests can be used to estimate the longitudinal aerodynamic characteristics, such as C_{m_α}, using the real ALFLEX vehicle. By using the aerodynamic pitching moment and lift coefficients estimated from the hanging flight test rather than those estimated from development wind-tunnel tests, and by assuming their variations to be negligibly small, the probability of exceeding the sink-rate requirement at touchdown was reduced to an acceptable level. Figure 9 shows RSS and Monte Carlo simulation results obtained by using the values of C_{m_α} and C_{L_α} identified by five DOF hanging flight tests. The probability of not satisfying the requirement is about 1.5%, as opposed to the previous 5% shown in Fig. 8b. These results were obtained prior to the first landing trial and enabled the program to proceed to free flight trials without changing the guidance and control laws and with confidence of successful landing. Figure 10 shows the flight-test results for the same variables. Comparing the flight-test results and numerical simulations, we recognized that the real test results corresponded to quite probable outcomes of the simulation tests (i.e., the test results were in regions where the density of simulation results were quite high). Postflight analysis indicated that the estimated derivatives of C_{m_α} and C_{L_α} were well within 1σ (Ref. 15).

From RSS analysis parameters influencing the final landing performance were identified, and the results were able to be used in planning corresponding ground tests and preliminary hanging flight tests to finally verify the design before the first landing flight. Because RSS only gives an approximate estimate of landing performance, Monte Carlo simulations that can account for the system's nonlinearity are necessary to derive reliable estimates of probability distributions of variables directly related to landing performance. In other words, the Monte Carlo simulation can give an estimate of the final mission achievement probability, which is the quantity to be maximized by the flight control system design. This clear design goal can contribute to the efficiency of the design process. This approach is similar to the concept of stochastic robustness.[20,21] Extension of this evaluation approach to a design problem will be discussed in Sec. V.

B. Flight-Test Results and Simulation Analysis After Flight Test

All 13 landing flights satisfied the landing performance requirements in Table 1. A typical example of obtained landing performance has been shown in Fig. 10. Deviations were small in spite of varying wind conditions. Figure 11 shows the wind conditions encountered in the 13 landing trials. Figure 12a shows the reference and actual longitudinal and lateral flight trajectories of the 13 landing trials before and around the time of touchdown. The lateral deviation is sufficiently small, and there is no obvious bias tendency with respect to the reference line, which is a straight extension of the runway center line. The longitudinal flight path, however, shows a repetitive tendency: a deviation of a few meters above the reference altitude at the end of preflare and a floating tendency at the final flare. According to the simulation conducted at the final FCP design tuning, the vehicle flew almost on the curved reference path under conditions of no wind and no error.

The cause of the repetitive error in the longitudinal path from the preflare to the final flare was investigated after the flight tests. The reasons are estimated to be as follows[10]:

1) Because of air data sensor position error, the EAS calculated onboard is about 3% less than the true value. This introduces a bias error in the vehicle's vertical acceleration response.

2) MLS sensor delay was estimated to be about 60 ms. In the design of final guidance law tuning, it was assumed to be 200 ms. This introduces an altitude navigation error in the beginning of the preflare phase.

Figure 12 shows an example simulation analysis from the error source investigation. It plots simulation results that explain the cause of the floating tendency of the vehicle. Although the EAS error and MLS delay time error were relatively large compared with their 3σ variations, the landing performance still had a high probability of meeting the design requirement as had been estimated. Needless to say, after the deterministic error sources and their values had been identified, the guidance law could have been tuned to improve the landing performance. However, the FCP was not modified throughout the 13 flight tests because we were convinced that the performance was within the design requirement and that the observed tendencies were not at all critical to the vehicle's safe flight.

To summarize the ALFLEX longitudinal guidance and control problem:

1) From simulation analyses, landing performance degradation caused by errors in the C_{m_α} and C_{L_α} estimates could occur such that requirements were not satisfied. Because aerodynamic data obtained from the preliminary hanging flight test were able to confirm the values of C_{m_α} and C_{L_α}, or reduce the width of their uncertainties, the program was able to proceed to the landing trials.

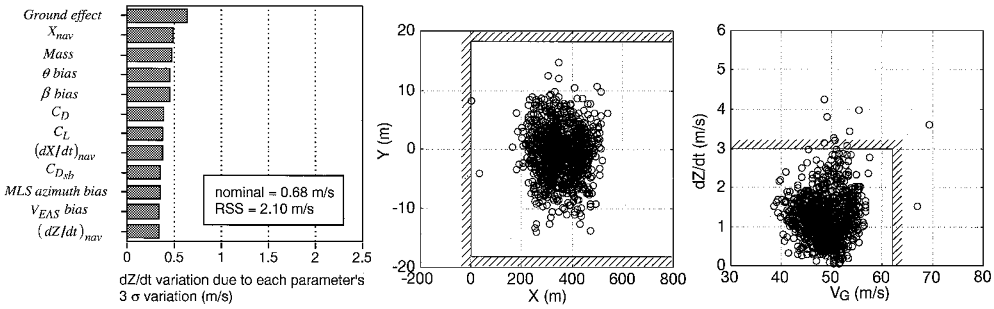

Fig. 9 Monte Carlo simulation results (after C_{m_α} and C_{L_α} variation reduction).

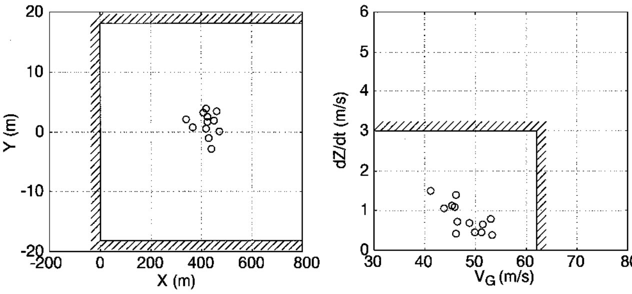

Fig. 10 Flight-test results corresponding to Figs. 8b and 9 Monte Carlo simulations.

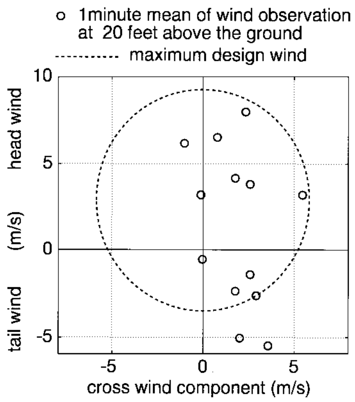

Fig. 11 Wind condition.

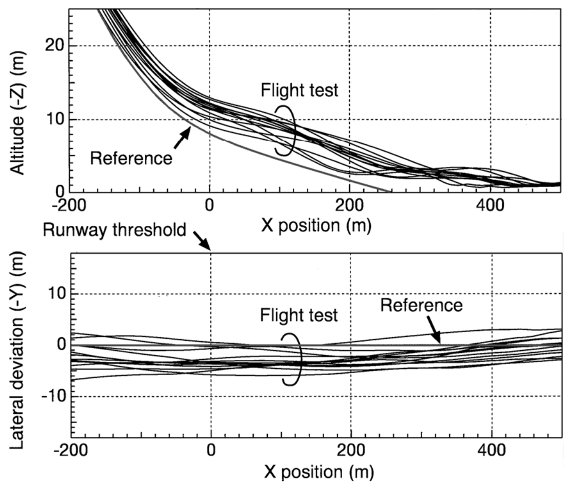

Fig. 12a Landing flight trajectories.

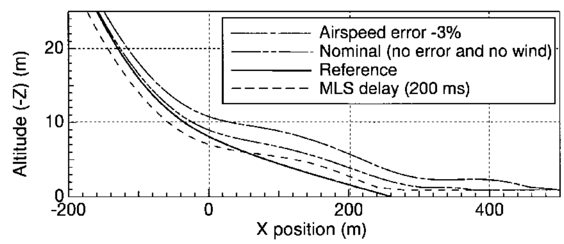

Fig. 12b Simulation analysis to reproduce the floating tendency.

However, HOPE-X will not have the benefit of such a special flight test to reduce aerodynamic data uncertainties, and significant improvements in the quality of wind-tunnel data are difficult to obtain. Therefore, the guidance and control laws should be reviewed.

2) Even though longitudinal aerodynamic derivative errors were reduced, sensitivity analysis and Monte Carlo simulation analysis showed that the longitudinal landing performance barely satisfies the requirement and is still sensitive to various errors. This result is in contrast to the lateral-directional landing performance, which has ample margin. As had been predicted to some extent, the vehicle experienced consistent and repetitive path-following error because of air data sensor error and navigation sensor delay error. Although landing performance was still within the requirement despite the error, an improvement in the guidance and control law was desired. In particular, ALFLEX's air data sensor probe is on top of the pitot boom, which is more advantageous than the ordinary probe position. HOPE-X will have pitot probes installed on the forebody like the U.S. space shuttle, which will be more prone to position error. The next section will discuss further investigation conducted after the flight test.

V. Post Flight-Test Guidance and Control Law Investigation and Review

To enhance robustness against uncertainties and sensor errors while maintaining the nominal landing performance, three types of modifications (I, II, and III) were considered. These modifications are basically minor changes, as shown in the block diagrams in Fig. 13.

A. Modification I: Guidance Feedback Gain Review by Stochastic Gain Tuning

In the design of the guidance laws, some stability margin had been retained to avoid coupling with rigid body rotational motion, and it was therefore possible to further fine tune or to increase the feedback gain to the limit to suppress the guidance error. Further tuning, however, can be effective only when various kinds of uncertainty have been sufficiently modeled. For this further tuning the stochastic robustness measure already discussed was extended to the design problem, where evaluation by Monte Carlo simulation was fully utilized. However, currently available design tools are limited, so that the design parameters were selected to be the most effective two gains, that is, the proportional and derivative gains, denoted by Kp and Kd, respectively, as shown in Fig. 6b.

In the process of gain tuning, adjustable parameters Kp and Kd are considered to be additional random variables whose stochastic properties are defined as independent and uniformly distributed. The range of each parameter, corresponding to areas to be searched, is defined appropriately. Among the 10,000 Monte Carlo simulations conducted, 2122 cases were unsatisfactory in that they did not satisfy the performance requirements (including uncontrollable cases), and Fig. 14 shows all unsatisfactory cases plotted on the Kp–Kd plane regardless of other random variables. Because Kp and Kd

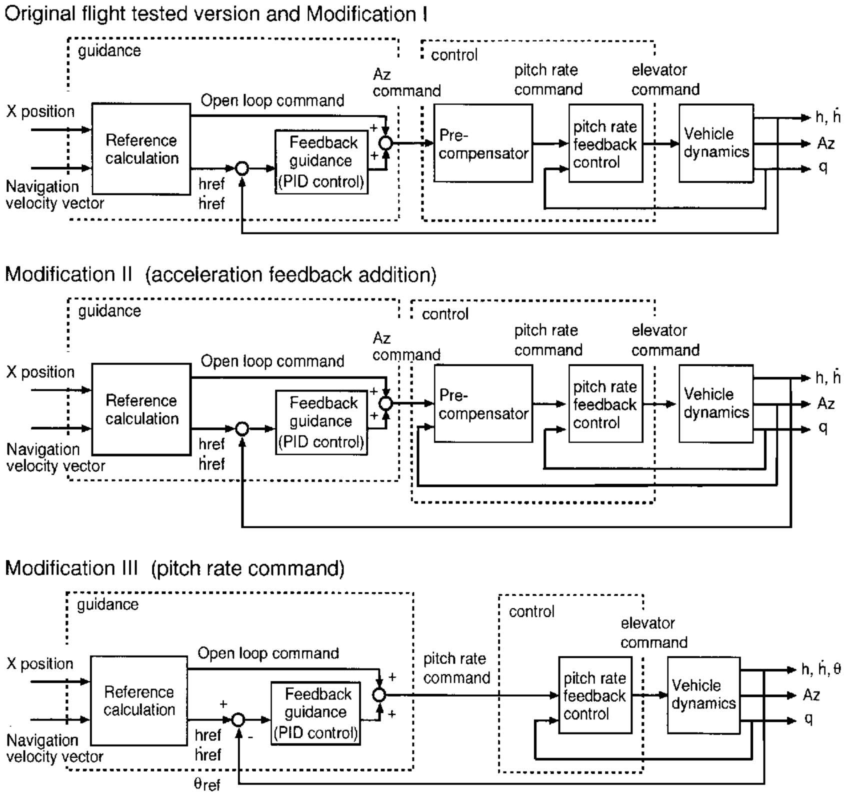

Fig. 13 Block diagrams of three types of modification.

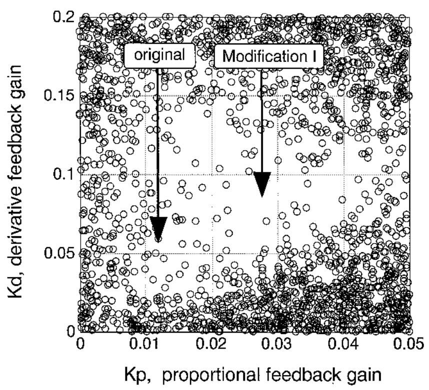

Fig. 14 Stochastic gain tuning for Modification I.

are distributed uniformly, the sparse areas in the figure indicate that the corresponding feedback gains are effective for mission achievement. In this figure, *original* indicates the point of the ALFLEX guidance gain, which seems to be not necessarily optimal. By inspection of the figure, the new values of Kp and Kd, 0.027 and 0.09, respectively, were assigned at the indicated point.

Figure 15 shows RSS and Monte Carlo simulation results using the new guidance gains. To allow direct comparison of performance with the earlier results in Figs. 8a and 8b, the stochastic properties of the vehicle are those derived prior to the hanging flight test, i.e., uncertainty includes the longitudinal aerodynamic derivatives C_{m_α} and C_{L_α}. The comparison shows a significant performance improvement, in that the probability of exceeding the mission requirement limit is reduced to approximately one-fifth of its original value. The design approach adopted here, gain tuning by stochastic robustness measure, could be called stochastic gain tuning.

B. Modification II: Acceleration Feedback Addition to Reduce Acceleration Response Error

One of the reasons that the landing trajectory is sensitive to longitudinal aerodynamic derivatives is that the aerodynamic changes affect the response to an acceleration command. Open-loop command in the preflare phase is basically derived for the vehicle to follow the reference trajectory using the vehicle's acceleration response in the nominal condition. For this reason the response change and sensor errors generate some disturbance through the mistuned open loop command. If acceleration feedback is added to compensate for the change in response, it would be effective in improving the performance robustness. In the ALFLEX GNC design, however, it was considered that in order to avoid a control/structure coupling problem it is better to have no acceleration feedback. Because the response change to be reduced here is for the low-frequency range, it can be compensated by acceleration feedback with an appropriately designed low-pass filter.

The acceleration feedback gain was designed using the MDM/MDP approach, and the guidance gains Kp and Kd were redesigned by the stochastic gain tuning method, as for the previous modification. Figure 16 shows the RSS and Monte Carlo simulation results of this modification. As in the preceding modification, the stochastic properties of the vehicle used are those prior to the hanging flight test so the performance can be compared with Figs. 8a, 8b, and 15. They show further performance improvement in that the probability of exceeding the sink-rate requirement limit becomes extremely small.

C. Modification III: Pitch-Rate Command

A pitch-rate command type guidance/control structure had already been discussed in the preliminary design of the ALFLEX GNC system. In the postflight design review the structure was reexamined using the final simulation model. Because ALFLEX longitudinal guidance and control uses pitch rate as a principal controlled variable for pitching motion, the same feedback loop transfer function for the pitch-rate command as that of the flight-tested version can be derived, which includes a precompensator for transforming the acceleration command to pitch-rate command. For the same reason the pitch-rate open-loop command and the acceleration open-loop command are interchangeable; the open-loop command designed for acceleration command can be transformed to a pitch-rate command in a more complex form, and vice versa. So the assessment should be based on which command is easier to design in order to obtain more robust performance. In fact, from the postflight design study with some trial and error, no significant improvement in landing performance compared with the original flight-tested version could be obtained.

Table 3 Stochastic landing performance, number of unsatisfactory cases among 1000 simulations[a]

Guidance and control law	Corresponding figure	$X < 0$ m	$dZ/dt > 3$ m/s	Number of cases, $V_G > 62$ m/s	$\|\Phi\| > 10$ deg and/or $\|\Psi\| > 8$ deg	Total number (probability estimate)
Flight-tested version	Fig. 8	8	39	12	2	51 (5%)
Flight-tested version (limited uncertainty)	Fig. 9	0	11	2	3	15 (1.5%)
Modification I	Fig. 15	0	8	0	3	10 (1%)
Modification II	Fig. 16	0	0	4	1	5 (0.5%)

[a]Among the landing performance requirement items, the air-speed condition is excluded.

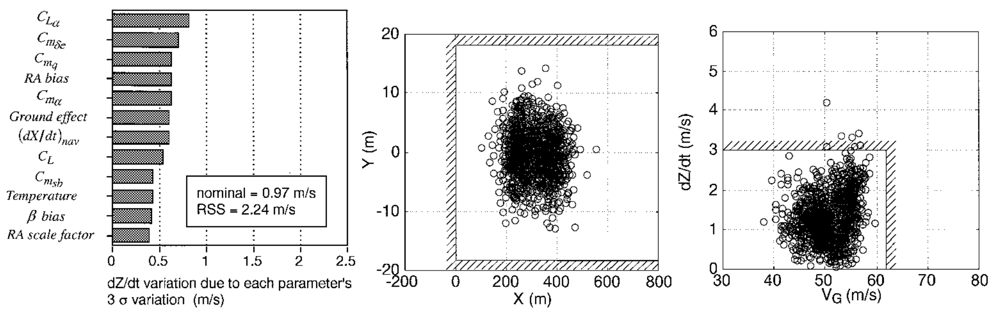

Fig. 15 Landing performance for Modification I (stochastic gain tuning for ALFLEX guidance feedback control).

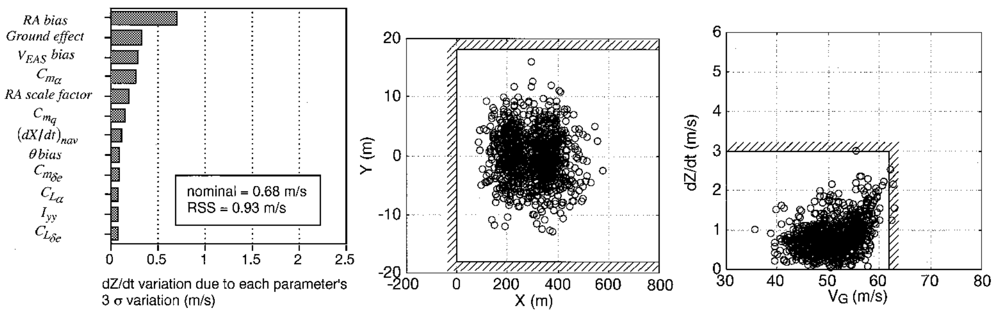

Fig. 16 Landing performance for Modification II (acceleration feedback addition to the precompensator).

The landing performances evaluated by Monte Carlo simulations are summarized in Table 3. Table 3 compares landing simulations in four cases: two cases using the flight-tested version of the guidance and control laws and Modifications I and II. These correspond to Figs. 8b, 9, 15, and 16. One of the flight-tested cases limits C_{m_α} and C_{L_α} uncertainty by using the five DOF hanging flight-test results, and all other cases use the same full uncertainty, i.e., the same 1000 combinations of uncertain parameters, except for C_{m_α} and C_{L_α}, were examined for each guidance and control law. In each case there are one or two occurrences of uncontrollable flight where the simulation exceeds the limit of the model's effective range caused by lateral-directional mode instability. Among the landing performance requirement parameters, touchdown position and sink rate are the most critical. Except for the flight-tested version with aerodynamic uncertainty, the probability of not touching down on the runway is not critical. As for the total number of unsatisfactory cases in Table 3, the air-speed requirement 59 m/s $> V_{EAS} >$ 43 m/s is excluded because it is not critical for safe landing. The total numbers of simulations that exceed the requirement demonstrate the robustness of each guidance and control law. Modification II is more robust than Modification I at some cost to robustness in touchdown ground speed. In any case Modifications I and II demonstrate some performance improvement, and they present solutions to the problem of longitudinal flight control design for the ongoing HOPE-X program. Monte Carlo simulation and stochastic gain tuning are essential tools in the analysis and synthesis.

VI. Conclusions

Because the vehicle's longitudinal reference path for horizontal landing is curved and path control becomes a tracking problem, not a regulator problem, changes of the flight control system response, or inner-loop response, easily affect the path-tracking performance through the open-loop command. Therefore, robust flight control design against uncertainties in vehicle dynamics and sensor errors is important. The ALFLEX longitudinal flight control system achieved this design requirement by adopting a unique control structure that enables the vehicle to possess quick acceleration response and thus permits a high feedback guidance gain. Although the high feedback guidance gain is useful in suppressing path error, the open-loop command and the vehicle's response error, caused by precompensator bias error and aerodynamic data error, themselves introduce some amount of path error. In fact, the ALFLEX simulation analysis and flight tests showed that the pitching moment uncertainty and air data sensor error influenced the landing performance. A design review conducted after the ALFLEX flight tests showed some performance improvements.

The results are summarized as follows:

1) The guidance gain of the flight-tested version of the longitudinal guidance and control laws had some margin for increase. Gain modification can be optimized by the method of stochastic gain tuning, which is an extension of stochastic robustness to the gain tuning problem.

2) Acceleration feedback added to the control law has a little effect on the performance robustness. Even with the structure modification, however, stochastic gain tuning is necessary to optimize the total guidance system.

3) Pitch-rate command was also reviewed as an alternative guidance command. There has been no evidence that using a pitch-rate command is better than using an acceleration command. As a result, the choice of acceleration as the longitudinal guidance/control interface variable in the ALFLEX design could be justified in the design review.

Through the design, development, and flight test we learned that simulation which includes uncertainty is very important for evaluating the GNC system. A sophisticated simulation tool was developed for the ALFLEX program. Monte Carlo simulation, which needs a certain amount of computational resources, can give a rational measure of probability of final mission achievement. This measure is useful in efficient GNC design and development. The stochastic gain tuning method, which optimizes the measure, has been demonstrated as a promising approach for designing the flight control system of a space vehicle.

Acknowledgments

Kawasaki Heavy Industries Co., Ltd., Fuji Heavy Industries Co., Ltd., and TOSHIBA participated in the program. The authors appreciate their collaboration. Masahiko Nagayasu of NAL and Hidehiko Nakayasu of NASDA are the project leader and subleader, respectively. Keiji Tanaka, Tetsuhiko Ueda, and Takatsugu Ono, all from NAL, are the technical leaders of the flight experiment system, vehicle system, and ground facilities, respectively.

References

[1]Kempel, R. W., "Developing and Flight Testing the HL-10 Lifting Body: Precursor to the Space Shuttle," NASA RP-1332, April 1994.

[2]"Flight Test Results Pertaining to the Space Shuttlecraft," NASA TM X-2101, June 1970.

[3]"Shuttle Performance, Lessons Learned," NASA CP-2283, March 1983.

[4]Tsikalas, G. M., "Space Shuttle Autoland Design," AIAA Paper 82-1604, Aug. 1982.

[5]Kafer, G. C., "Space Shuttle Entry/Landing Flight Control Design Description," AIAA Paper 82-1601, Aug. 1982.

[6]Bayle, G. P., "Entry Flight Control Off-Nominal Design Consideration," AIAA Paper 82-1602, Aug. 1982.

[7]Ashkenas, I. L., Hoh, R. H., and Teper, G. L., "Analysis of Shuttle Orbiter Approach and Landing," AIAA Paper 82-1607, Aug. 1982.

[8]Myers, T. T., McRuer, D. T., and Johnston, D. E., "Space Shuttle Flying Qualities and Flight Control System Assessment," AIAA Paper 82-1608, Aug. 1982.

[9]Powers, B. G., "Space Shuttle Longitudinal Landing Flying Qualities," *Journal of Guidance, Control, and Dynamics*, Vol. 9, No. 5, 1986, pp. 566–572.

[10]*Proceedings of the ALFLEX Symposium*, National Aerospace Laboratory/National Space Development Agency of Japan, NAL SP-39T, Univ. of New South Wales, Sydney, Australia, 1997, pp. 1–172.

[11]Miyazawa, Y., Ishikawa, K., Motoda, T., Izumi, T., Sagisaka, M., Hata, T., and Onuma, H., "Flight Control System for the Automatic Landing Flight Experiment," AIAA Paper 96-3782, July 1996.

[12]Izumi, T., Sagisaka, M., Nakayasu, H., Miyazawa, Y., Yanagihara, M., and Ono, T., "Flight Test Results of Automatic Landing Flight Experiment (ALFLEX)," *Proceedings of the 48th International Astronautical Congress*, International Astronautical Federation, IAF-97-V.4.06, Oct. 1997.

[13]Miyazawa, Y., Ishikawa, K., and Fujii, K., "Guidance and Control Law for Automatic Landing Flight Experiment of Reentry Space Vehicle," AIAA Paper 93-3818, Aug. 1993.

[14]Ohno, M., Yamaguchi, Y., Hata, T., Takahama, M., Miyazawa, Y., and Izumi, T., "Robust Flight Control Law Design for Automatic Landing Flight Experiment," *Proceedings of the 14th International Federation of Automatic Control (IFAC) Symposium on Automatic Control in Aerospace*, Elsevier Science, Oxford, Aug. 1998, pp. 259–264.

[15]Yanagihara, M., Shigemi, M., and Suito, T., "Estimating Aerodynamic Characteristics of the ALFLEX Vehicle Using Flight Test Data," AIAA Paper 97-3485, Aug. 1997.

[16]Tsukamoto, T., Yanagihara, M., and Nagayasu, M., "ALFLEX Five Degrees of Freedom Hanging Flight Test," AIAA Paper 97-3484, Aug. 1997.

[17]NAL/NASDA ALFLEX Group, "Flight Simulation Model for Automatic Landing Flight Experiment," National Aerospace Lab., Tokyo, TR TR-1252, Oct. 1994 (in Japanese).

[18]Motoda, T., Miyazawa, Y., Ishikawa, K., and Izumi, T., "ALFLEX Flight Simulation Analysis and Flight Testing," AIAA Paper 98-0301, Jan. 1998.

[19]Rockwell International Space Systems Group, "STS-1 Aerodynamic Design Data Book," NASA CR-160903, Nov. 1980.

[20]Ray, L. R., and Stengel, R. F., "Application of Stochastic Robustness to Aircraft Control Systems," *Journal of Guidance, Control, and Dynamics*, Vol. 14, No. 6, 1991, pp. 1251–1259.

[21]Marrison, C. I., and Stengel, R. F., "Design of Robust Control Systems for Hypersonic Aircraft," *Journal of Guidance, Control, and Dynamics*, Vol. 21, No. 1, 1998, pp. 58–63.